Al-Azhar University Civil Engineering Research Magazine (CERM)
Vol. (40) No. (3) July, 2018

Flexural behavior of fiber reinforced post-tension concrete beams under cyclic loading

A. El-Thakeb[1], H.El-Esnawi[2], A.Hafiz[3], M.A.Asran [4]

[1]Prof. Civil Engineering Dept., Faculty of Engineering, Al-Azhar University, Cairo, Egypt
[2]Ass.Prof. Civil Engineering Dept., Faculty of Engineering, Al-Azhar University, Cairo, Egypt
[3]Lecturer Civil Engineering Dept., Faculty of Engineering, Al-Azhar University, Cairo, Egypt
[4] Lecturer Assistant, Civil Engineering Dept., Higher Technological Institute 10th of Ramadan City, Egypt

الملخص

يتضمن البحث دراسة سلوك الكمرات الخرسانية المسلحة لاحقة الشد بسيطة الارتكاز المضاف عليها الياف حديديه بنسب مختلفه من حجم الخرسانه المعرضة لاحمال ترددية ناتجة من تأثير حملان كلا منهما فى ثلث بحر الكمرهوقد إستندت الدراسة علي النتائج المعملية التي تم اجراؤها علي4 كمرة مسلحة تشتمل علي متغيرات رئيسي وهو الياف الحديد الذى له تأثير علي سلوك الكمرات فى مقاومة اجهادات الشد المتولده نتيجة العزوم. جميع الكمرات تم إختبارها حتي الانهيار وتم تسجيل القراءات والملاحظات ورصد أشكال الشروخ وحمل الانهير الأقصي ورسم منحنيات وذلك بغرض دراسة تأثير استخدام الياف الحديد فى مقاومة اجهادات الشد للكمرات لاحقة الشد تحت تاثير الاحمال الترددية.

Abstract.

This paper presents an experimental study on the behavior of post-tensioned concrete beams with variable discontinuous fibers' content. Four half scale R-shaped post-tensioned simple beams were cast and tested in two points bending under the effect of a repeated load using a displacement control system up to failure. The test parameters were the fibers' content. Key test results showed considerable enhancement in the crack distribution, crack width and spacing, concrete tensile strength and flexural stiffness in all beams with steel fibrous concrete. The latter aspects were directly proportional to the steel fibers' contents. Furthermore, fibrous concrete beams also demonstrated enhanced ductility and energy absorption, which reached the highest values for steel fibrous concrete specimens. Generally, it can be concluded that steel fibers proved to have higher structural efficiency when used in the tested specimens.

1. Introduction.

Pre-stressing is a technique that has been widely used for decades in all sorts of concrete structures. Its ability to minimize reinforcement congestion, decrease deflection, and control cracking under service loads has made it a widely popular choice for large spans and for the precast industry.

The current edition of the ACI Building Code (ACI 318–2008) [1] now recognizes Four classes of pre-stressed flexural members, A, B, C, and D. Under full service load. The dividing lines between the four classes are based on nominal tensile stresses in the pre-compressed tensile zone. The ACI Building Code (ACI 318–2008) [1] limited the design of these members to the full pre-stressed case. Which have allowable tensile stress equal zero. Partially pre-stressed concrete offers several advantages over fully pre-stressed. *The overall objective* of this study was to determine the viability of unbonded partially post-tensioned concrete members under the impact of cyclic loading.

The difference between fully and partially pre-stressed concrete beams is referred to the allow- able permissible tension stresses [1]. Fully pre-stressing is de- fined as a complete elimination of tensile stresses in members at full service load or allow small tension stresses, which can be resisted by concrete only, while partially pre-stressing allow for higher tension stresses in concrete and cracking under full service loads [2,3]. In this research, the partially pre-stressed concrete beams were achieved with a combination of pre- stressed and non-pre-stressed reinforcement while fully pre-stressed concrete beams contained pre-stressed reinforcement only.

Manalip et al. [3], studied the behavior of the compression zone of reinforced and pre-stressed HSC elements and concluded that HSC has a brittle behavior in case of specimens subjected to axial compression, while different behavior was observed for reinforced or pre-stressed beams. It was also re- ported that use of HSC results in doubling the plastic rotation capacity, for reinforced or pre-stressed concrete beams subjected to pure flexural stresses.

Xiao and Ma [4] investigated the seismic performance of HSC beams in moment resisting frame structures. Two large scale HSC and two counterpart normal-strength concrete model beams were tested under cyclic shear and double bending. Studies showed that both high-strength and normal-strength concrete beams developed ductile flexural responses. The HSC beams exhibited increased capacity and improved hysteretic performance compared to normal-strength concrete beams.

2. Experimental Program.

2.1. Description of specimens.

A total of four half scale unbonded post-tensioned simple beams were tested under cyclic load up to failure. The main parameter among the tested specimens is the pre-compression value which can also be definite as the partially pre-stressed ratio (PPR).

Figs. (1), show the specimen's dimensions, internal reinforcement, cable profile, and support arrangement for all tested specimens. All tested specimens had a typical R-shaped cross-section and equal spans. All beams had the same dimensions with a total length of 4700 mm, clear span of 4500 mm, beam width of 150 mm, and an overall height of 350 mm, as shown in the figures. All beams were designed to have the same ultimate moment capacity. Cable profiles are the same for all beams. In order to prevent the occurrence of shear failure prior to the flexural failure, the shear reinforcement of all specimens were consisting of two 10 mm vertical branches with horizontally spaced 100 mm at the maximum shear zone, and 150mm spacing at zero shear zone. In addition, the transverse reinforcement of the compression zone consisted of 10 mm diameter bars, and variable tensile reinforcement. All the pre-stressing cables comprised of seven wires with a nominal diameter 0.6 in which equal to 15.24 mm. The main parameter among the tested specimens is the volume of fiber content. The four tested specimens were coded as following B1-25-PP-0.73-0, B2-25-PP-0.73-0.5, B3-25-PP-0.73-1and B4-25-PP-0.73-1.5, and only one cable in order to simulate the post tensioning system. Table (1). Details of tested specimens

Details of specimens	**Beam specimens**			
	B1-25-PP-0.73-0	B2-25-PP-0.73-0.5	B3-25-PP-0.73-1	B4-25-PP-0.73-1.5
Top RFT	2Φ10	2Φ10	2Φ10	2Φ10
Bottom RFT	2Φ10	2Φ10	2Φ10	2Φ10
Shear RFT	10Φ10/m	10Φ10/m	10Φ10/m	10Φ10/m
PT strand	0.6”	0.6”	0.6”	0.6”
PPR ratio	0.73	0.73	0.73	0.73
Fiber %	0	0.5	1	1.5

Specimen's details, mechanical properties for reinforcing bars, and mechanical properties of used materials are listed in Table(1)&(2)

* Where (B1, B2, B3----) are the beams codes which are given as the beam number.

* The value (25) refers to concrete compressive strength.

* PP refers to fully or partially post-tensioned respectively.

* The value (0.73) refers to (PPR).

Table (2). Mechanical properties of concrete.

Mechanical properties	**Beam specimens**			
	B1-25-PP-0.73-0	B2-25-PP-0.73-0.5	B3-25-PP-0.73-1	B4-25-PP-0.73-1.5
F'_c (mPa)	24.94	25.11	25.26	26.88
F_t (mPa)	2.9	3.1	3.8	4.1

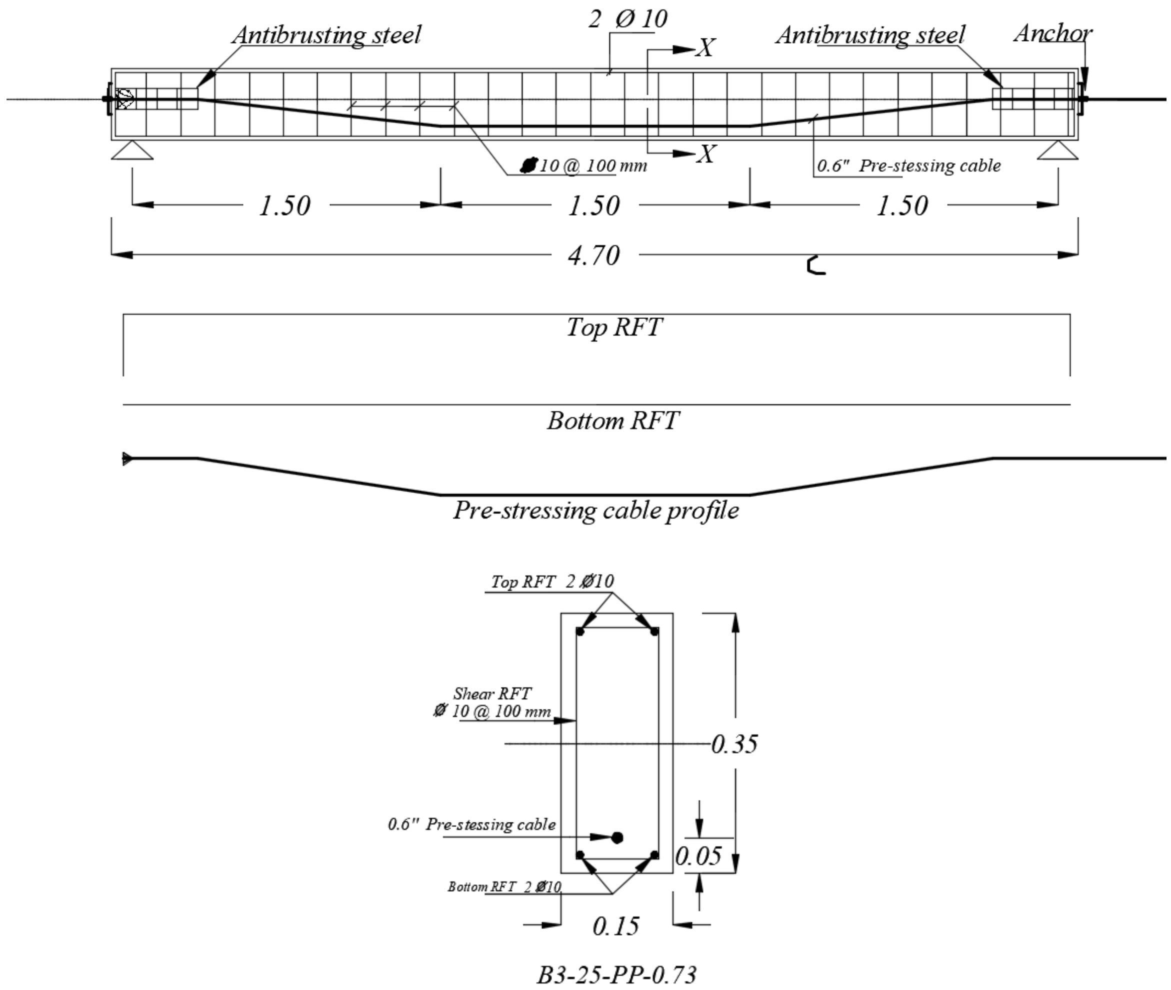

Fig.(1) Reinforcement details of specimen's

2.2. Specimen's fabrication and pre-stressing process.

Plywood forms were prepared for casting the concrete in the laboratory of AL-AZHAR University. All forms had the same dimensions. The steel reinforcement cages were prepared and put into the forms. Corrugated plastic ducts for strands were accurately and symmetrically installed about mid-span in the forms. Two end-bearing plates were positioned at the two ends of all beams to distribute the pre-stressing force over all the cross sections of the beams in order to avoid any cracks in the anchorage zone. The concrete was compacted for two minutes after casting, using an electrical poker vibrator, followed by water curing and covering with polythene sheeting for one week. For control purposes, 6 cylinders with 150 mm diameter and 300 mm height, were cast alongside the specimens from the same concrete batch and were cured with the specimens. The cylinders were tested before pre-stressing and at the same day of testing the beams. Table (2) shows the average cylinder strength after two months from casting of the concrete. Fig (2) shows the forms, reinforcement cages and curing process.

The pre-stressing force was applied at 75% of the ultimate strength of the strands. One mono barrel anchor was installed at one end of the beams since all beams had one live end and deed end. A calibrated hydraulic jack was used in the pre-stressing process. The stressing forces were transferred from the hydraulic jack to the strands along four equal stages ranging from 25% to 100% of the required force. The force in the strands was measured through the elongation of the strands which was measured at every stressing stage. Pre-stressing presses was done immediately before testing to avoid occurrence of long term losses. Fig (3) shows the pre-stressing process.

2.3. Instrumentation.

Two Linear Variable Distance Transducers (LVDTs) with 0.01 mm accuracy were used to measure the mid-span deflections of all beams, as shown in Fig. (4). The electrical resistance strain gauges, which were attached to steel bars and concrete, were connected to a data acquisition system to record the data. Finally, the data were collected using a data acquisition system and ''lab view'' software at a rate of 2 sample per seconds.

2.4. Test setup and loading procedure.

Fig. (4) Shows the details of the test set-up. It should be noted that the test arrangement was symmetrical about the mid-span section of all beams. Each beam was loaded in two loading points bending. The beams were subjected to a uni-directional cyclic loading up to failure, using a hydraulic actuator of 250 kN capacity. The load was applied on the beams using a stroke displacement control system, which divided the machine load that was applied through a steel spreader beam 1.5 m in length, as shown in the figure. The cyclic loading was achieved by increasing the stroke with 2 mm increments each two cycles until failure. As shown in fig (5).

Fig (2) Forms, reinforcement cages and curing process.

Fig (3) Pre-stressing process.

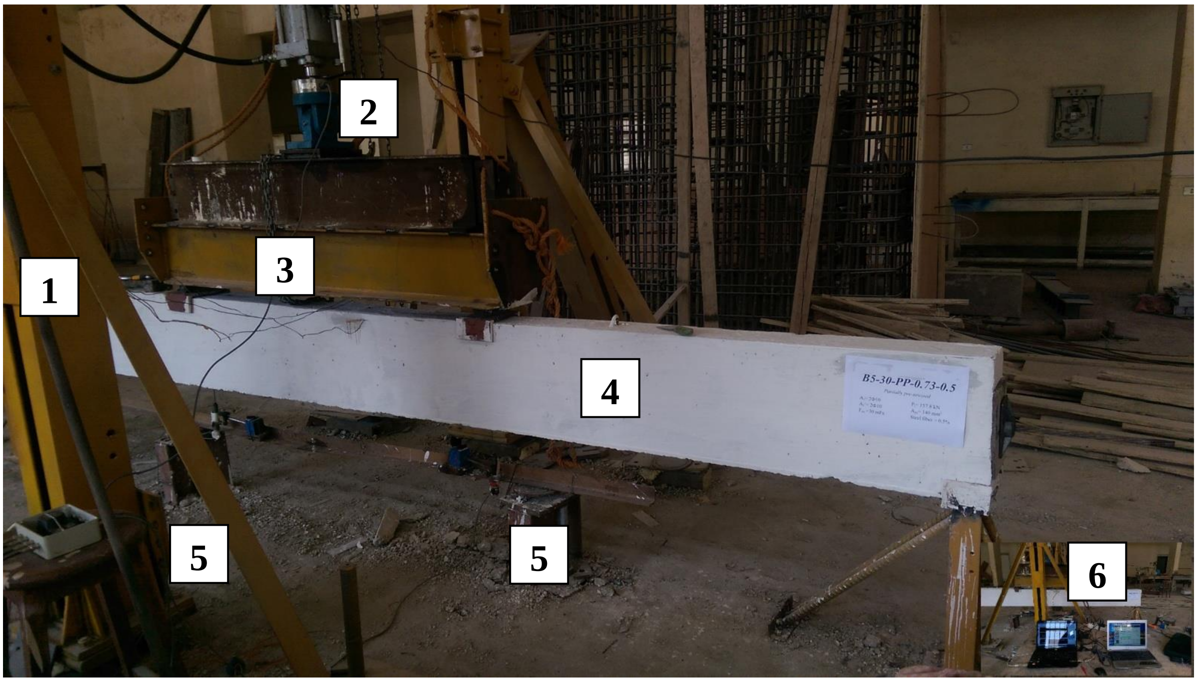

1) Loading frame
2) Hydraulic actuator.
3) Steel spreader beam
4) Tested specimen
5) LVDT
6) Data acquisition system

Fig (4) Test set up.

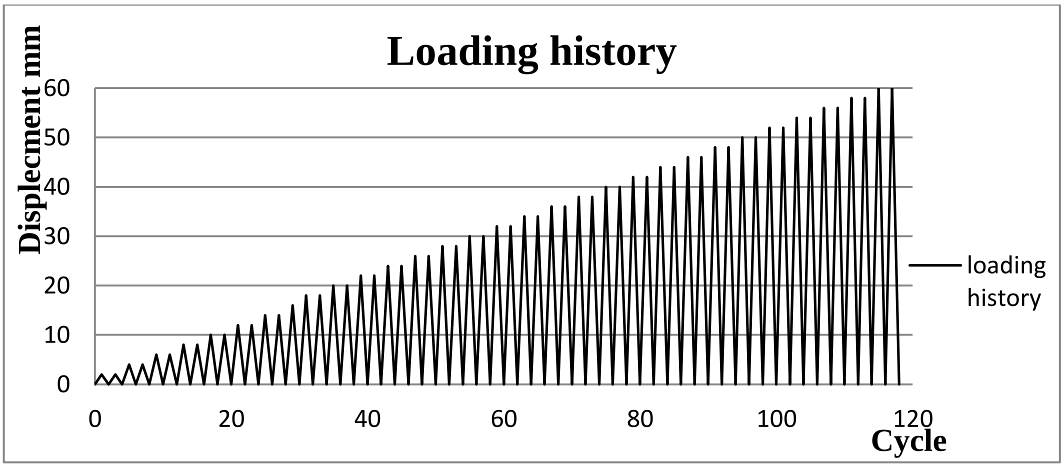

Fig (5) Loading history

3. Test results and discussion.

3.1 Crack pattern and failure mode.

Fig. (6) Shows the crack patterns at failure of all tested beams and Table (3) Summarize the details of the test process of all beams. On the other hand, Fig. (7) Shows the total load versus the mid span deflection of all tested beams.

1. Flexural cracks initiated at pure bending sections of beams. During the +14Δy loading process, flexure-shear cracks could not be observed. Flexural cracks penetrating over the full depth of beam sections. After that, the existing cracks kept on increasing with occurrence of new cracks. Finally, more vertical cracks and a few inclined cracks could be observed around the mid-span sections of beams.

2. When the width of cracks was less than 0.3 mm, cracks at the bottom of post-tensioned beams were almost closed, accompanied by very small residual deformation during the unloading, which indicated that the pre-stressed members behaved with large capacities in crack and deformation restoring.
3. For all post-tensioned beams, the crack propagation followed similar traditional flexural patterns in simple beams and the first tension cracks appeared in the constant moment zone. In addition, large number of cracks with small crack width was observed. In fact, Conventional ductile flexural failure occurred due to cutting of the main bottom steel followed by concrete crushing.
4. Failure patterns for all specimens were dominated by flexural effects. It could be observed that concrete crushed and spalled off at pure bending zone with a buckling of longitudinal steel bars. All failures occurred under extremely large deformations.

Fig. (6) Crack patterns at failure of all tested beams

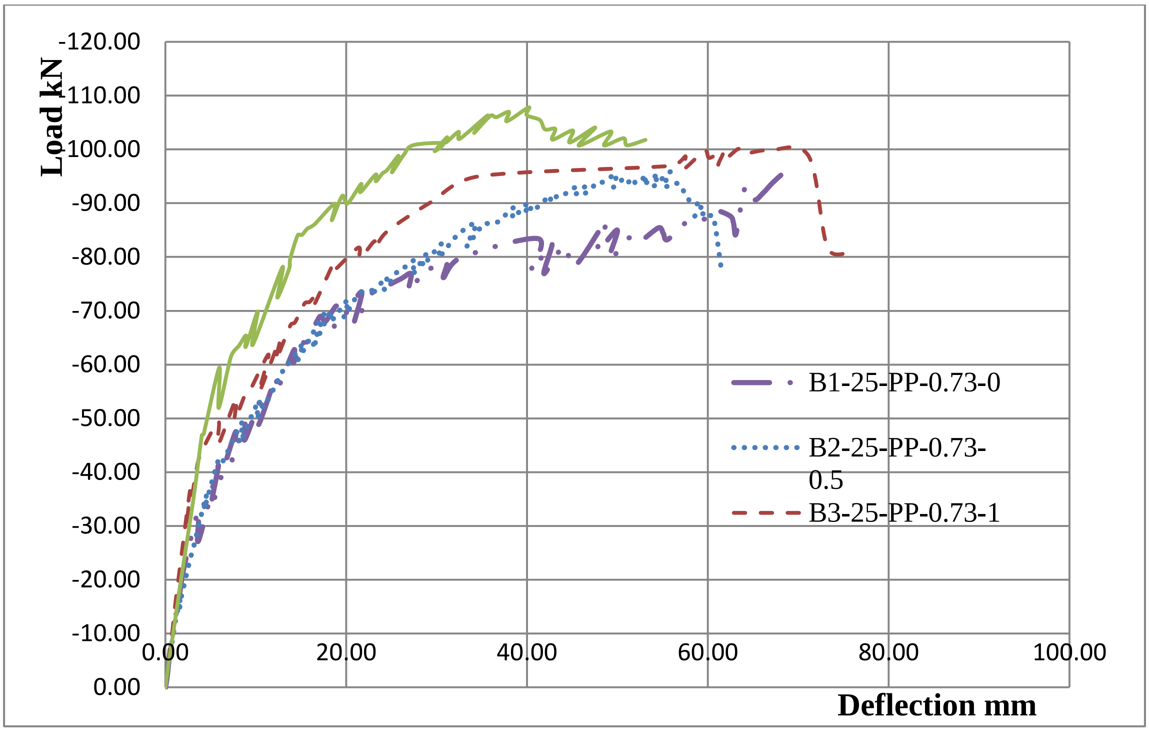

Fig. (7) Total load versus the mid span deflection of all the tested beams.

Table (3) Summarize the details of the test process of all the tested beams

Parameters	**Beam specimens**			
	B1-25-PP-0.73-0	B2-25-PP-0.73-0.5	B3-25-PP-0.73-1	B4-25-PP-0.73-1.5
Cracking load Pcr (kN)	26.5	28	31	36.4
Yielding load Py (kN)	72.1	78.5	91	96
Max. load Pmax (kN)	95.86	101.1	107.8	109.6
Ultimate load Pu (kN)	81.48	85.93	91.63	93.16
Failure cycle	72	78	84	96
Failure patterns	Many parallel vertical cracks at pure bending especially at the mid-span of the beams where the moments are large. A few inclined cracks could be observed at flexure-shear sections and Concrete crushed and spalled off at pure bending sections and loading points with cutting of steel bars at tension side and buckling of longitudinal steel bars at compression side.			

3.2. Skeleton curves.

Skeleton curves shown in Fig. (7) Are envelopes of hysteresis curves. The followings can be obtained from these figures:

1. Skeleton curves of the four beams could be divided into three phases: the elastic phase, the yield phase, and the ultimate phase.
2. In the elastic phase, the relationships between loads and mid-span deflections in skeleton curves are basically linear before concrete cracking. After the cracking of specimens, the skeleton curves become more curved. When the specimens yield, evident inflexion points could be observed. In the yield phase, slit increase in the vertical loads take place with increasing displacements.
3. An increase in cracking load in B4-25-PP-0.73-1.5 is due to high fiber ratio content. Also an obvious decrease in ultimate displacement and high load carrying capacity could be observed.
4. An increase in yield loads and yield displacements due to a higher amount of fiber ratio content could be observed in B3-25-PP-0.73-1and B4-25-PP-0.73-1.5. Also an obvious decrease in cracking load could be observed in B1-25-PP-0.73-0.
5. The load carrying capacity of B1-25-PP-0.73-0 (no fiber content) and B4-25-PP-0.73-1.5 (highest fiber content).quite close to each other, indicating that relatively low addition of steel fiber has little effect on the load carrying capacity of beams.
6. An obvious decrease in cracking load, yield load, ultimate displacement, and load-carrying capacity in control beam is probably due to very absence of steel fiber.
7. The Failure of control beam occurs earlier than beams containing steel fiber in cycles. A descending branch could be observed after the yielding of reinforcement steel, indicating that steel fiber had a contribution to the load-carrying capacity of post-tensioned beams, while however enhancing the displacement ductility of fiber content beams.

3.3. Deformation restoring capacity.

Structures are always in the elasto-plastic range during strong dynamic loading. The deformation restoring capacity and residual deformation directly affect the rehabilitation and serviceability of structures. In this paper, the residual deformation ratio, which is defined as $\Delta r / \Delta u$ [5], is used as a key index for evaluating the deformation restoring capacity of beam specimens. Here, Δr is the residual displacement after unloading and Δu is equal to the maximum displacement for skeleton curves without the descending part or equal to the displacement corresponding to 85% maximum load in the descending part of the skeleton curves. The parameters for the restoring behavior of beams are presented in Table (4).

Table (4).parameters for the restoring behavior of beams.

parameters	Beam specimens			
	B1-25-PP-0.73-0	B2-25-PP-0.73-0.5	B3-25-PP-0.73-1	B4-25-PP-0.73-1.5
Δr (mm)	44.89	33.5	38.35	26.07
Δu (mm)	75.41	63.2	75.2	52.14
Δr / Δu	0.6	0.54	0.51	0.5

As shown in the table, the following could be obtained:

1. The residual deformation ratios of the control beam are about 0.6, indicating that beam display relatively small deformation restoring capacities.

2. The residual deformation ratio of beams containing steel fiber are about 0.54-0.5 indicating that beam display relatively large deformation restoring capacities than that of control beam. That is due to the use of steel fiber.
3. The residual deformation ratio of B4-25-PP-0.73-1.5 during loading is a little than other beams at corresponding loading stages. Conclusions can be drawn that using steel fiber makes obvious contribution to the deformation restoring capacity beams.
4. The residual deformation ratio of B2-25-PP-0.73-0.5, B3-25-PP-0.73-1 and B4-25-PP-0.73-1.5 is higher than that of control beam, which indicates that an increase in steel fiber ratio has obvious influence on the deformation restoring capacity of pre-stressed beams.
5. Higher increase in the steel fiber content would lead to a decrease in the deformation restoring capacity by comparing the residual deformation ratios of B2-25-PP-0.73-0.5, B3-25-PP-0.73-1 and B4-25-PP-0.73-1.5. it obviously affected the overall beam behavior in term of cracking load, load carrying capacity, and ultimate deformation.
6. The residual deformation ratios of beams containing steel fiber are obviously lower than those of the control beams at corresponding loading stages, reflecting that the use of steel fiber results in a reduction in residual deformation. This also means that the fiber reinforced concrete behaves in a better deformation-restoring manner, thus they are much more convenient for rehabilitation in comparison with control beams.

3.4. Displacement ductility.

Displacement ductility is used as an important index for the dynamic evaluation of structures. The ductility coefficient μ, representing the ratio of ultimate displacement (Δu) to yield displacement (Δy), is defined as $\Delta u/\Delta y$ [5]. Δy is equal to the displacement corresponding to the yielding of the beam specimens. The measured ductility coefficients of beams at each characteristic point are presented in Table (5).

Table (5) Measured ductility coefficients of tested beams.

parameters	Beam specimens			
	B1-25-PP-0.73-0	B2-25-PP-0.73-0.5	B3-25-PP-0.73-1	B4-25-PP-0.73-1.5
Δy (mm)	30.4	23.23	26.47	19
Δu (mm)	75.41	63.2	75.2	52.14
$\mu = \Delta y / \Delta u$	2.48	2.72	2.84	2.86

The following conclusions can be drawn:

1. The maximum displacement ductility coefficient (2.86) is achieved in B4-25-PP-0.73-1.5, while the minimum displacement ductility coefficient (2.48) occurs in specimen B1-25-PP-0.73-0. Conclusions can be drawn that the beams containing steel fiber behave in a more ductile manner than control beams.
2. It also can be observed that in fiber reinforced concrete the displacement ductility could be increased by increasing fiber ratio content by comparing the ductility coefficients of control beams.
3. By comparing B2-25-PP-0.73-0.5, B3-25-PP-0.73-1 and B4-25-PP-0.73-1.5, it could be observed that the displacement ductility of the pre-stressed beams could be improved significantly by using steel fiber.

4. Conclusions.

Experimental uni-directional cyclic loading tests of fully and partially post-tensioned beams are conducted in this paper. Based on the results of this study, the following conclusions can be stated:

1. Most of post-tensioned beams reach higher capacity than their designed ultimate capacity. Such as specimens B3-25-PP-0.73-1 and B4-25-PP-0.73-1.5their ultimate failure load increased by 12.8 kN and 14.6 kN respectively. The increase was regarded to the effect of steel fiber.
2. The cracking load of beams containing steel fiber is much higher than that of control beam. Beams containing steel fiber cracked at 28, 31 and 36.4 kN, while the control beams cracking load ranged is 26 kN. This can be regarded to the using of steel fiber.
3. Residual deformation in control beam was much higher than that of beams containing steel fiber. The residual deformation ratios of beams containing steel fiber range from 0. 5 to 0.54. The residual deformation ratios of the control beam (about 0.6, indicating that the beam behaves with relatively low deformation restoring capacity.
4. Fiber reinforced post-tensioned beams exhibited an increase in displacement ductility coefficient ranged from 10% to 17% higher than control beam, indicating that Fiber reinforced post-tensioned beams behave more ductile manner.
5. The stiffness degradation of fiber reinforced post-tensioned beams mainly was much lower than that of control beams. Indicated that increasing fiber ratio decrease the stiffness degradation.

5. Reference.

1. ACI Committee 318. Building Code Requirements for Structural Concrete (ACI 318–2008) and Commentary (ACI 318–2008). American Concrete Institute, 2008
2. A.E. Naaman, Presressed Concrete Analysis and Design, McGraw Hill, NY, 1982, p. 670
3. H. Manalip, M. Pinglot, M. Lorrain, Behavior of the compressed zone of reinforced and prestressed high strength concrete beams, ACI Journal 149 (1994) 209–226 (SP149-12).
4. Xiao Yan, Ma Rui. Seismic behavior of high strength concrete beams. The Structural Design of Tall Buildings 1998;7:73–90.
5. Weichen Xue_, Liang Li, Bin Cheng, Jie Li. The reversed cyclic load tests of normal and pre-stressed concrete beam. Engineering Structures 30 (2008) 1014–1023